Science Immunology
AAAS

Supplementary Materials for

Immune checkpoint blockade sensitivity and progression-free survival associates with baseline CD8$^+$ T cell clone size and cytotoxicity

Robert A. Watson *et al*.

Corresponding author: Benjamin P. Fairfax, benjamin.fairfax@oncology.ox.ac.uk

Sci. Immunol. **6**, eabj8825 (2021)
DOI: 10.1126/sciimmunol.abj8825

The PDF file includes:

Figs. S1 to S7

Other Supplementary Material for this manuscript includes the following:

Tables S1 to S13

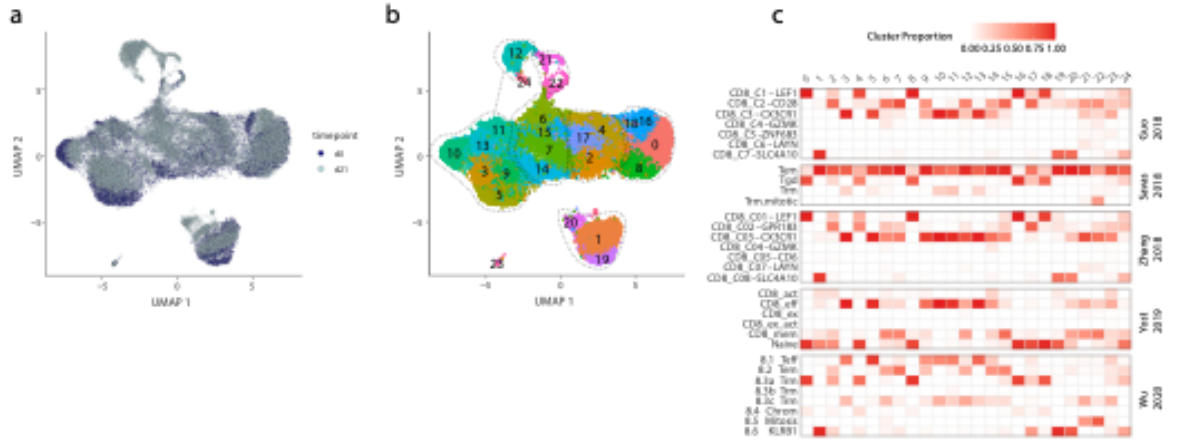
a
b
c
UMAP 1
UMAP 2
timepoint
d
Subsets
Guo et al 2018
Savas et al 2018
Zhang et al 2018
Yost et al 2019
Wu et al 2020
Clusters
Naive
CD8_C1-LEF1
CD8_C01-LEF1
Naive
0,8,16,18
CM
CD8_C2-CD28
CD8_C02-GPR183
CD8_mem
2,4,17
EM
CD8_C4-GZMK
Tem
CD8_C04-GZMK
8.2-Tem
6,7,14,15
Effector
CD8_C3-CX3CR1
CD8_C03-CX3CR1
CD8_eff
8.1-Teff
3,5,9,10,11,12,13
MAIT
CD8_C7-SLC4A10
CD8_C08-SLC4A10
8.6-KLRB1
1,19,23
Mitotic
Tmitotic
8.5-Mitosis
21,22
Other
CD8_C5-ZNF683
CD8_C6-LAYN
Tgd,Trm
CD8_C05-CD6
CD8_C06-CD160
CD8_C07-LAYN
CD8_act,CD8_ex
CD8_ex_act
8.3-Trm,
8.4-Chrom
23,24
f
nUMI
Normalized MKI67 Expression
Naive
CM
EM
Effector
Mitotic
γδ
MAIT
e
Naive
CM
EM
Effector
Mitotic
MAIT
Other
naive
CM
EM
Effector
MAIT
g
Phase
G1
G2M
S
Cell Cycle Phase Proportion
h
Cytotoxicity Score

Supplementary Figure 1: **Workflow for CD8$^+$ T cell subset assignments. (a)** UMAP distribution of cells from pre-treatment (d0) and day 21 on-treatment (d21) samples. **(b)** UMAP visualisation of 25 Seurat clusters generated at a FindClusters resolution of 1.5. **(c)** Heatmap of assigned subset identities for each Seurat cluster using external cancer patient single-cell RNAseq datasets as a reference*(12, 13, 39–41)* . For each cell, SingleR was used to cross-match its expression profile to that of one of the subsets in each reference set. The proportion of cells in each cluster that were assigned a particular identity from each reference set is represented by the intensity of shading (between 0 and 1). **(d)** Summary table of subset identities for each reference set and assigned identities for each cluster based on the best match from the SingleR analysis. **(e)** Phylogenetic tree for each Seurat cluster coloured by assigned subset showing similarity between clusters within the same subset. **(f)** Violin plot showing the nUMI (left) and normalised *MKI67* expression (right) per cell across each of the seven CD8$^+$ T cell subsets. **(g)** Bar plot of the proportion of cells in each stage of the cell cycle, assigned using the CellCycleScoring function in Seurat, across each subset. **(h)** Cytotoxicity score (based on expression of the 50 most *IFNG*-correlating genes, Supplementary Table S5) across each subset.

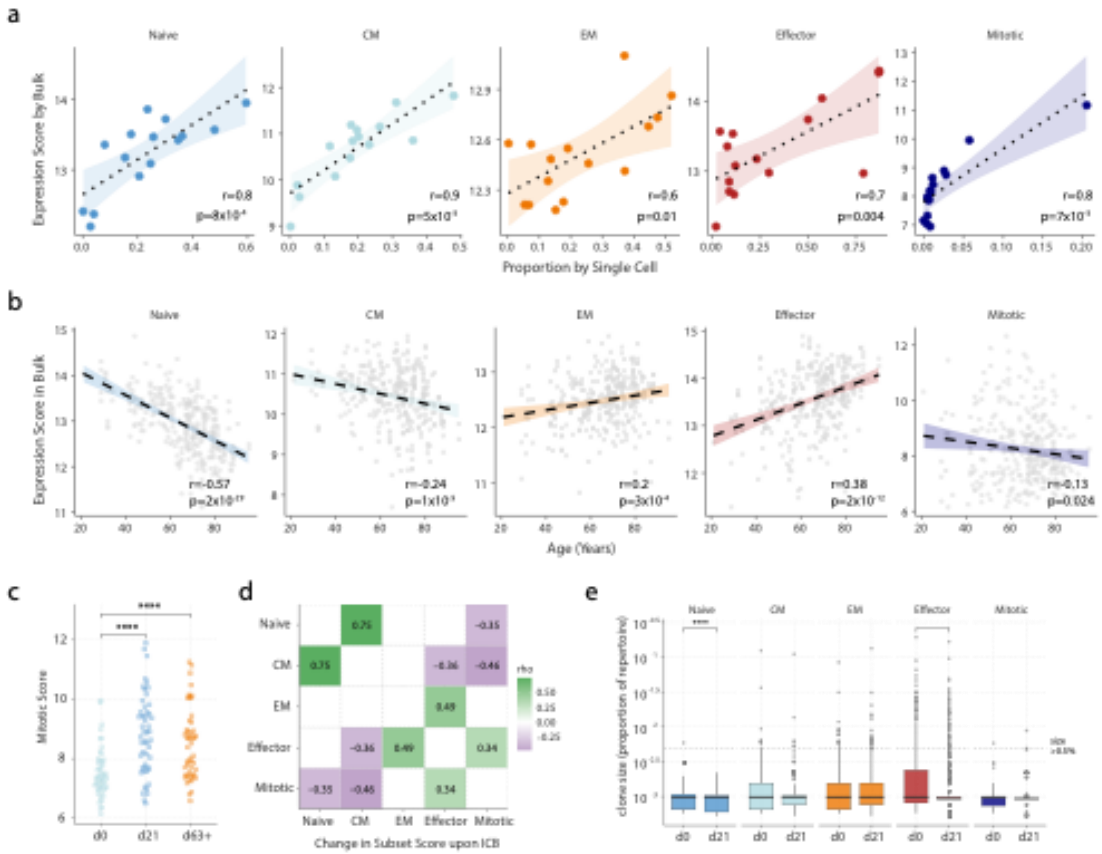
a
Naive
CM
EM
Effector
Mitotic
Expression Score by Bulk
Proportion by Single Cell
r=0.8
p=8x10⁻⁴
r=0.9
p=5x10⁻⁵
r=0.6
p=0.01
r=0.7
p=0.004
r=0.8
p=7x10⁻⁴
b
Expression Score in Bulk
Age (Years)
r=-0.57
p=2x10⁻¹⁷
r=-0.24
p=1x10⁻³
r=0.2
p=3x10⁻⁴
r=0.38
p=2x10⁻¹²
r=-0.13
p=0.024
c
Mitotic Score
d0
d21
d63+
d
Naive
CM
EM
Effector
Mitotic
rho
Change in Subset Score upon ICB
e
clone size (proportion of repertoire)
d0
d21

Supplementary Figure 2: **Inference of subset proportions and phenotype. (a)** Correlation between subset proportions for each single-cell sample and scores calculated for each subset using bulk RNAseq data of $CD8^+$ T cells. For 15/16 of the samples used for single-cell RNAseq, bulk RNAseq on the purified $CD8^+$ T cells was also performed. A list of the top 20 discriminating markers for each subset was generated using FindAllMarkers function from the Seurat R package (Materials and Methods, Downstream expression analysis) in the single-cell data for all d0 cells, and separately for all cells at d21 post-ICB. The overlapping genes were retained as markers of each cell subset irrespective of treatment, and the geometric mean expression for each set of genes was calculated using normalised bulk RNAseq data, thus generating subset scores for each bulk RNAseq sample. Pearson's correlation was used to determine the accuracy of this scoring approach for each subset. **(b)** As a further validation of the bulk RNAseq scores, subset scores across n=399 samples were correlated against participant age. Pearson's R and p values are labelled. **(c)** Changes in mitotic scores at d0, d21 or day 63+ (d63+) of treatment (n=49 individuals, two-sided Wilcoxon signed-rank test). **(d)** Heatmap of Spearman's rho values for correlations between bulk subset scores; filled boxes represent adjusted p-value <0.05 upon Bonferroni's correction. **(e)** Change in clonal size with major phenotype in the given subset at d0 and d21 (Wilcoxon rank-sum test). For each clone, the subset in which most of its members were present was designated as the predominant phenotype for that clone; clones equally distributed across multiple subsets were excluded. Clones above the dotted line represent large clones occupying size greater than 0.5% of the repertoire.

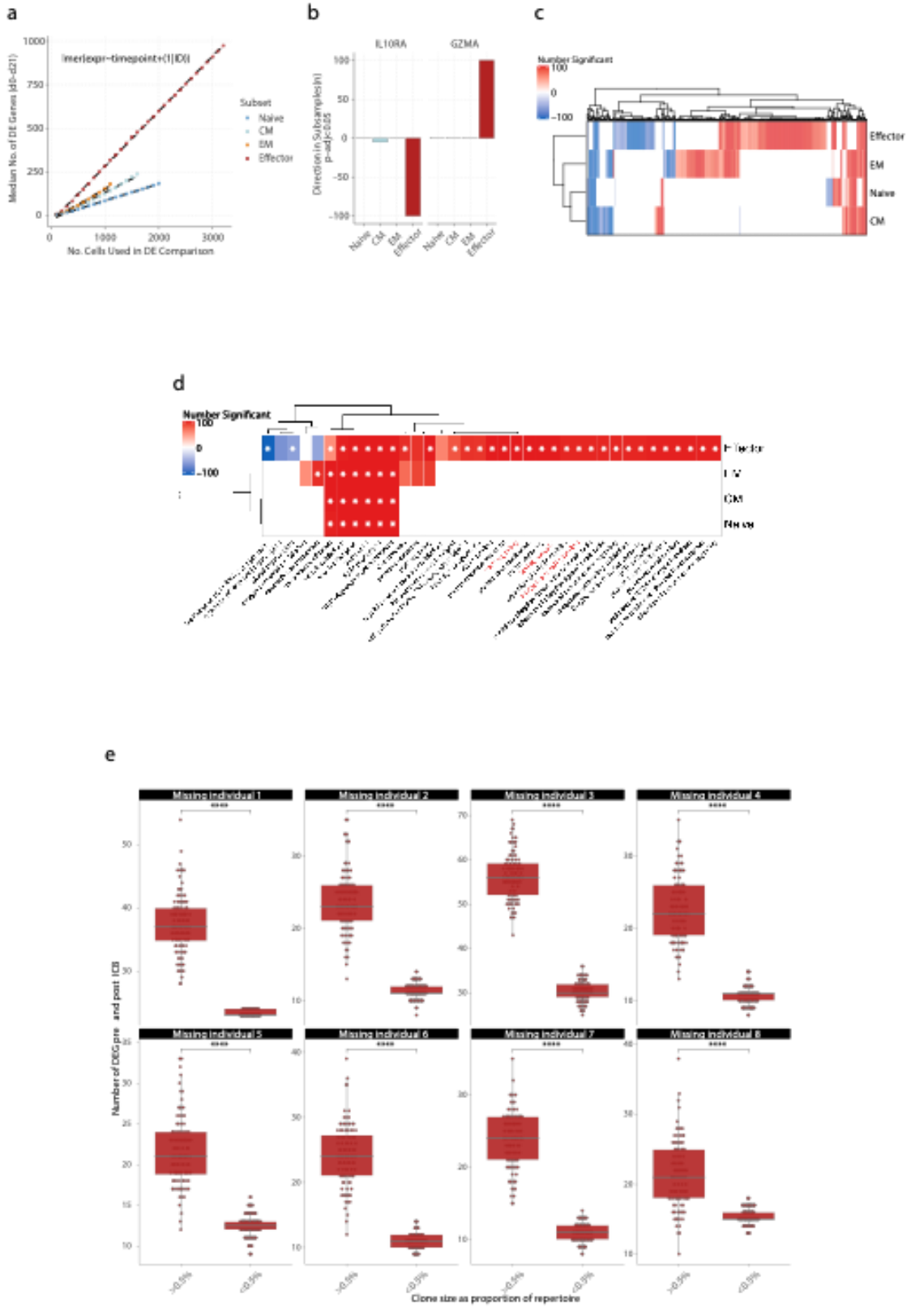
a
b
c
d
e
Median No. of DE Genes (d0-d21)
No. Cells Used in DE Comparison
Subset
Naive
CM
EM
Effector
IL10RA
GZMA
Direction in Subsample(n)
p-adj<0.05
Number Significant
Missing Individual 1
Missing Individual 2
Missing Individual 3
Missing Individual 4
Missing Individual 5
Missing Individual 6
Missing Individual 7
Missing Individual 8
Number of DEGs pre and post ICB
Clone size as proportion of repertoire

Supplementary Figure 3. Differential expression analysis across subsets and clone sizes. **(a)** Median number of differentially expressed (DE) genes across 21 days of ICB in conventional T cell subsets, as per Fig 3a but using the annotated linear mixed-effects model instead of the *FindMarkers* Seurat function to identify significantly modulated genes (Bonferroni's adjusted p-value <0.05). At each n-value for number of cells, there was a significant difference across the subsets in the number of DE genes ($p<0.0001$, Wilcoxon rank-sum test). **(b)** Differential modulation of *IL10RA* and *GZMA* across each subset using *FindMarkers* bootstraps. The number of times each of the specified genes was detected as significantly up- or downregulated across 100 bootstraps was plotted per subset (subsample of n=1100 cells, direction represents increased or decreased expression following ICB). **(c)** Heatmap of DE genes across each subset, detected in greater than 50/100 *FindMarkers* bootstraps. Intensity of shading indicates how many bootstraps the gene was detected in, and colour represents whether the gene was significantly up- or downregulated. **(d)** Heatmap of induced or suppressed GOBP pathways modulated in each subset, in more than 50/100 *FindMarkers* bootstraps; selected pathways highlighted in red. Pathways marked with an asterisk* represent those also found using an equivalent approach based on DE genes detected by the mixed linear model. **(e**) Number of differentially expressed genes pre- and post- treatment for large vs small ECs (red) sequentially omitting one individual each time. The EC cluster was subsampled to a constant size and the analysis bootstrapped 100x (Wilcoxon rank-sum test).

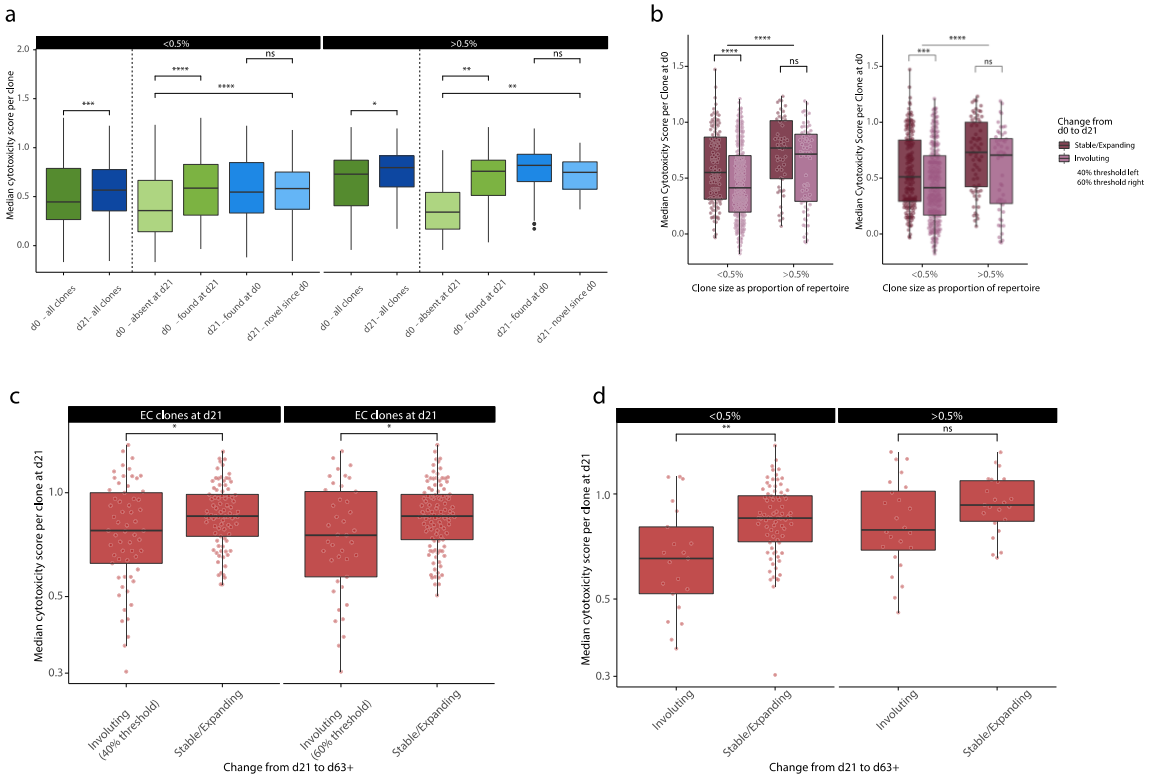
a
<0.5%
>0.5%
Median cytotoxicity score per clone
d0 - all clones
d21 - all clones
d0 - absent at d21
d0 - found at d21
d21 - found at d0
d21 - novel since d0
b
Median Cytotoxicity Score per Clone at d0
Clone size as proportion of repertoire
Change from d0 to d21
Stable/Expanding
Involuting
40% threshold left
60% threshold right
c
EC clones at d21
Median cytotoxicity score per clone at d21
Involuting (40% threshold)
Stable/Expanding
Involuting (60% threshold)
Change from d21 to d63+
d
Change from d21 to d63+

Supplementary Figure 4. Cytotoxic clones demonstrate propensity to persist post-ICB treatment. (a) Median cytotoxicity per clone for those found at both d0/d21 versus just at one timepoint, relative to all clones at d0 and d21. Clones were separated based on clonal size using a cut-off of 0.5% of the repertoire to denote large from small. **(b)** Median cytotoxicity per clone for those present at d0 that subsequently expand/remain stable (dark purple) or involute (light purple) by d21. Clones are separated based on size using a cut-off of 0.5% of the repertoire to denote large from small. Here, involuting clones are defined as those which are either 40% (left panel) or 60% (right panel) smaller at d21 compared to d0, whilst expanding/stable clones are those which, at d21, are within 40% or 60% of their baseline size, or have increased in size (**Materials and Methods, Clonal definitions, size and emergence vs involution**). **(c)** Median cytotoxicity score per clone across EC clones found at d21 that subsequently expand/remain stable or involute by d63+. Here, involuting clones are defined as those which are either 40% (left panel) or 60% (right panel) smaller at d63+ compared to d21, whilst expanding/stable clones are those which, at d63+, are within 40% or 60% of their d21 size, or have increased in size. **(d)** Median cytotoxicity per clone for EC clones found at d21 that are stable/expanding or involuting by d63+, separated based on clonal size using a cut-off of 0.5% of the repertoire to denote large from small. Wilcoxon rank-sum tests used for all comparisons unless otherwise stated.

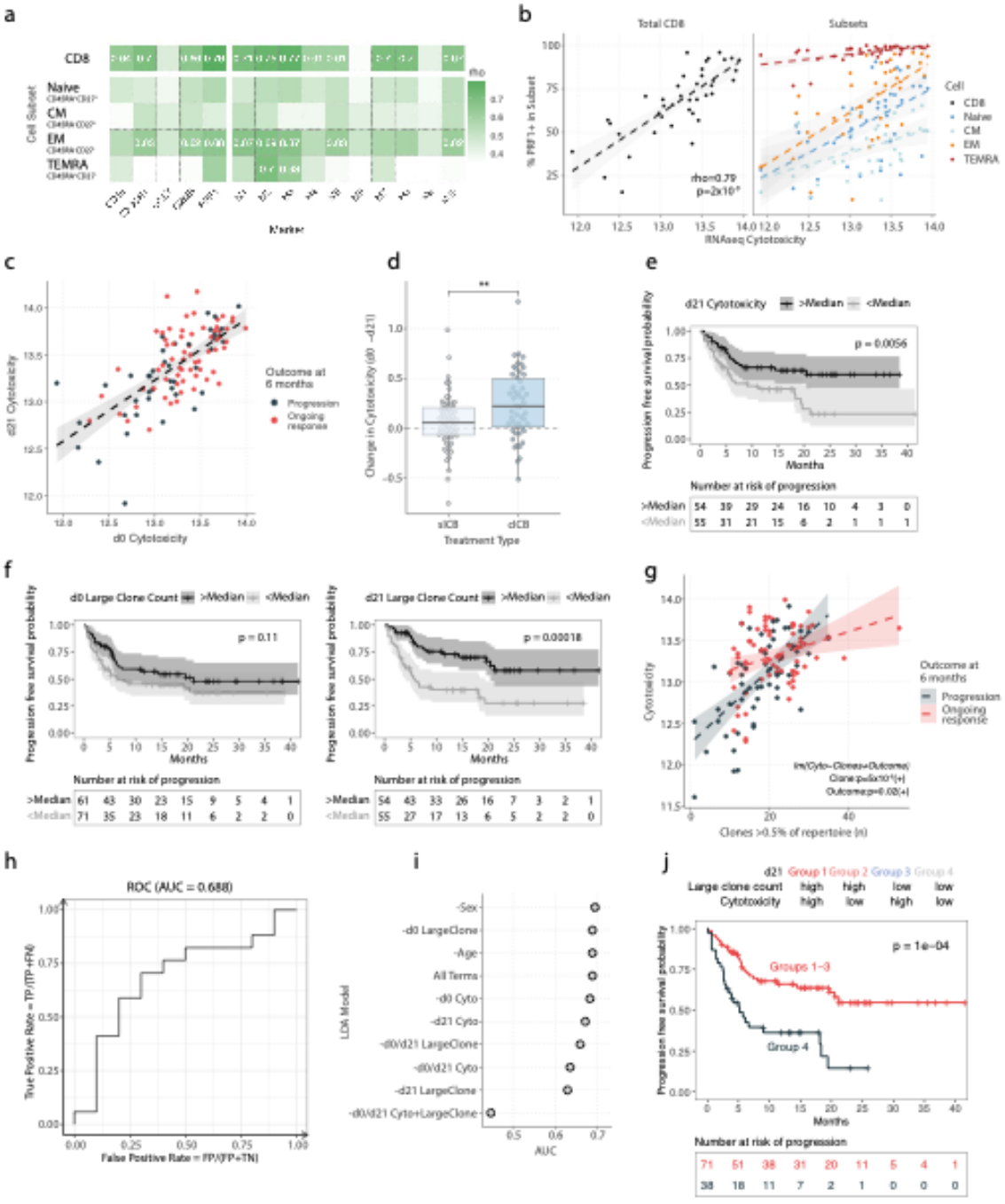
a
CD8
Naive
CM
EM
TEMRA
Cell Subset
rho
Marker
b
Total CD8
Subsets
% PRF1+ in Subset
rho=0.79
p=2x10⁻⁷
RNAseq Cytotoxicity
Cell
CD8
Naive
CM
EM
TEMRA
c
d21 Cytotoxicity
d0 Cytotoxicity
Outcome at 6 months
Progression
Ongoing response
d
Change in Cytotoxicity (d0 - d21)
**
sICB
cICB
Treatment Type
e
d21 Cytotoxicity >Median <Median
p = 0.0056
Progression free survival probability
Months
Number at risk of progression
>Median 54 39 29 24 16 10 4 3 0
<Median 55 31 21 15 6 2 1 1 1
f
d0 Large Clone Count >Median <Median
p = 0.11
d21 Large Clone Count >Median <Median
p = 0.00018
Progression free survival probability
Months
Number at risk of progression
>Median 61 43 30 23 15 9 5 4 1
<Median 71 35 23 18 11 6 2 2 0
>Median 54 43 33 26 16 7 3 2 1
<Median 55 27 17 13 6 5 2 2 0
g
Cytotoxicity
Clones >0.5% of repertoire (n)
lm(Cyto~Clones+Outcome)
Clone p=5x10⁻⁵(+)
Outcome p=0.02(+)
Outcome at 6 months
Progression
Ongoing response
h
ROC (AUC = 0.688)
True Positive Rate = TP/(TP+FN)
False Positive Rate = FP/(FP+TN)
i
-Sex
-d0 LargeClone
-Age
All Terms
-d0 Cyto
-d21 Cyto
-d0/d21 LargeClone
-d0/d21 Cyto
-d21 LargeClone
-d0/d21 Cyto+LargeClone
LOK Model
AUC
j
d21 Group 1 Group 2 Group 3 Group 4
Large clone count high high low low
Cytotoxicity high low high low
p = 1e-04
Groups 1–3
Group 4
Progression free survival probability
Months
Number at risk of progression
71 51 38 31 20 11 5 4 1
38 18 11 7 2 1 0 0 0

Supplementary Figure 5. $CD8^+$ cytotoxicity associations with flow cytometry, TCR analysis and clinical outcomes. (a) Heatmap of Spearman's correlations between bulk RNA-seq cytotoxicity and cytotoxic protein expression by flow cytometry across all $CD8^+$ T cells, or within $CD8^+$ cell subsets (n=20 d0 and 20 d21 samples; gating indicated on axis). M1-M10 refers to combinatorial gates of cytotoxic proteins; all gating listed in Supplementary Table 11. The top 10 Spearman's rho values are displayed in the heatmap. **(b)** Spearman's correlation between bulk RNA-seq cytotoxicity and % $PRF1^+$ cells across all $CD8^+$ T cells (left) or within subsets (right). **(c)** Correlation between cytotoxicity at d0 and d21 (n=106 patients, Spearman's rank test). **(d)** Change in cytotoxicity in bulk cohort between d0-d21 based on ICB treatment type (n=106 patients, Wilcoxon rank-sum test). **(e-f)** Kaplan-Meier curve of progression-free survival in patients with d21 cytotoxicity above and below median **(e)**, or d0 (left) and d21 (right) large clone count above and below median **(f)** (n=132 patients or 109 patients at d0 or d21 respectively, two-sided log-rank test). **(g)** Linear effect model testing for correlation between d0 cytotoxicity, and large clone count and six-month clinical outcome, controlling for both as covariates (n=132 patients, positivity or negativity of estimate value indicated in brackets). **(h)** Receiver operating characteristic plot for a linear discriminant analysis (LDA) model for six-month clinical outcome, incorporating d0 and d21 large clone count and cytotoxicity, age and sex (n=106 patients). Individuals were randomly separated into independent training (n=78) and test (n=28) sets for cross-validation. **(i)** Area under curve (AUC) values for the LDA model in (h) upon omitting various predictor variables. **(j)** Progression free survival in patients separated by a combination of d21 large clone count and cytotoxicity (above/below median) (n=109, two-sided log-rank test).

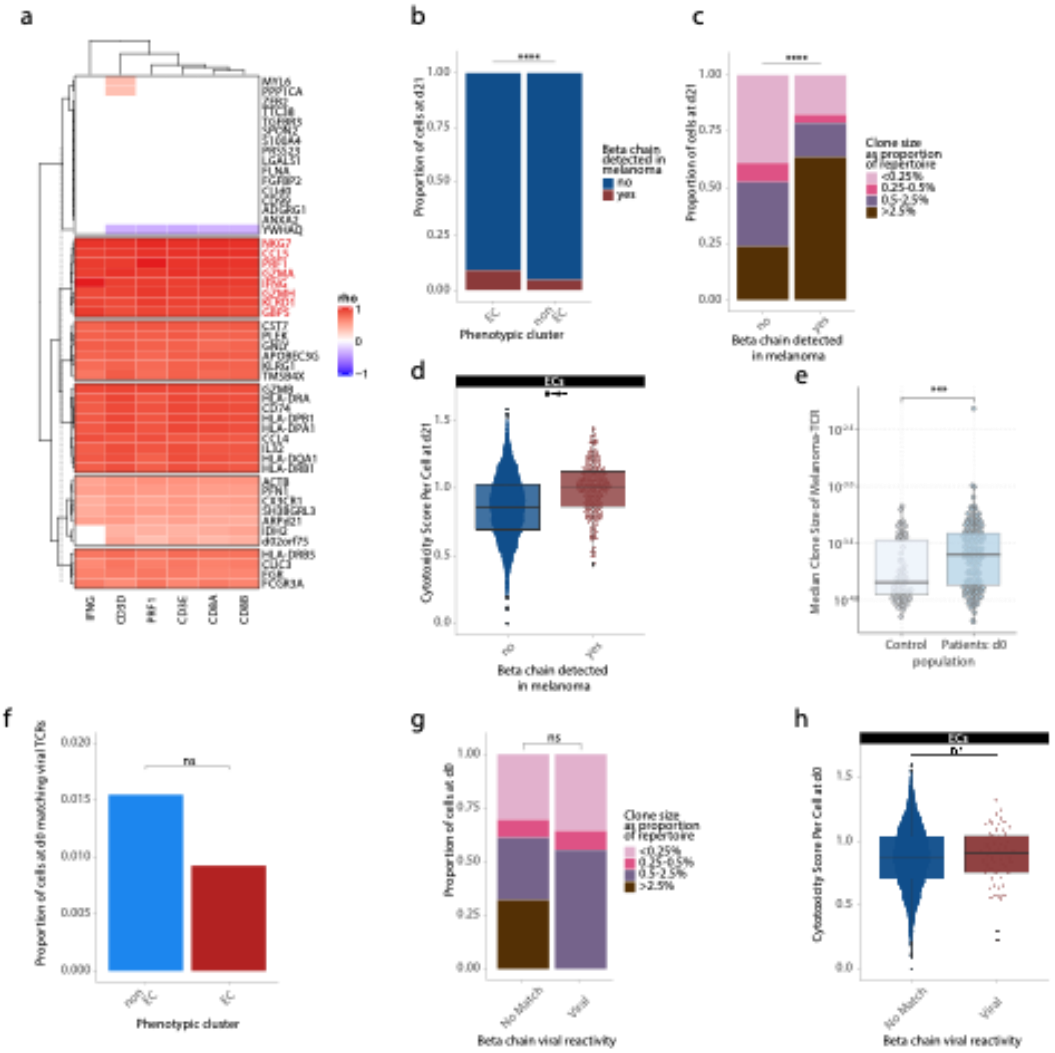
a
b
c
d
e
f
g
h
Phenotypic cluster
Beta chain detected in melanoma
Clone size as proportion of repertoire
Proportion of cells at d21
Cytotoxicity Score Per Cell at d21
Median Clone Size of Melanoma TCR
Control
Patients: d0
population
Proportion of cells at d0 matching viral TCRs
Proportion of cells at d0
Beta chain viral reactivity
No Match
Viral
ns

Supplementary Figure 6. Intratumoral analysis of T cell clonality and cytotoxicity. (a) Heatmap of Spearman's correlations based on tumour RNAseq data from Riaz et al. 2017*(25)* between *CD3D, CD3E, CD8A, CD8B, IFNG* and *PRF1* gene expression and 50 genes used in the calculation of peripheral cytotoxicity score, with the selected module of most-correlated genes used in the calculation of intratumoral T cell cytotoxicity highlighted in red. **(b)** Proportion of ECs compared to non-ECs at d21 that carry a tumour-associated TCRB chain (TA-TCRB), as identified by TCRseq of resected melanomas by Pruessman et al. 2020*(26)* (Fisher's exact test). **(c)** ECs at d21 that are either carrying a TA-TCRB or not, separated by clonal size; Fisher's exact test for the proportion of large clones (>0.5%) compared to small clones carrying/not-carrying a TA-TCRB. **(d)** Cytotoxicity scores of ECs at d21 categorised by whether they carry a TA-TCRB chain or not. **(e)** TCRB chains were matched with the TCR sequences in the bulk cohort and the median clone size of matching clones per individual was compared between healthy controls and melanoma patients. **(f-h)** TCR chains from the single-cell VDJ data were matched with viral TCR sequences from VDJdb and the relative subset enrichment **(f**; Fisher's exact test**)**, clonal size groupings in ECs **(g**; Fisher's exact test for proportion of clones >0.5% across groups) and cellular cytotoxicity in ECs **(h)** was similarly compared between viral-matching and non-matching cells. Wilcoxon rank-sum tests used for all comparisons unless otherwise stated.

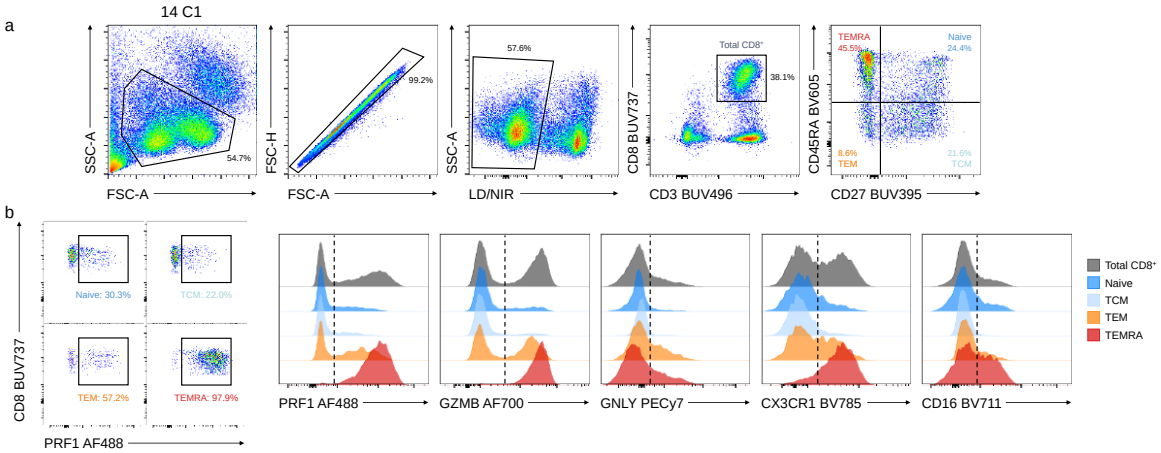
a
14 C1
SSC-A
FSC-A
54.7%
FSC-H
FSC-A
99.2%
SSC-A
LD/NIR
57.6%
CD8 BUV737
CD3 BUV496
Total CD8⁺
38.1%
CD45RA BV605
CD27 BUV395
TEMRA
45.5%
Naive
24.4%
8.6%
TEM
21.6%
TCM
b
CD8 BUV737
PRF1 AF488
Naive: 30.3%
TCM: 22.0%
TEM: 57.2%
TEMRA: 97.9%
PRF1 AF488
GZMB AF700
GNLY PECy7
CX3CR1 BV785
CD16 BV711
Total CD8⁺
Naive
TCM
TEM
TEMRA

Supplementary Figure 7. Representative plots for flow cytometry validation of in silico cytotoxicity scoring in CD8 T cells. (**a**) Representative dot plots showing gating strategy for live $CD8^+$ T cells and canonical subsets. $CD8^+$ T cells were gated as cells, singlets, live, $CD3^+$ $CD8^+$ events respectively, followed by CD27 and CD45RA-based discrimination of Naive, Central Memory (TCM), Effector Memory (TEM) and Terminal Effector Memory re-expressing CD45RA (TEMRA) subsets. (**b**) Expression of PRF1 (left; representative dot plots) and other cytotoxic markers (right; representative histograms) across the different subsets and the total $CD8^+$ T cell population.